A Clinical Study Comparing the Diagnostic Performance of Assist Strain Ratio Against Manual Strain Ratio in Ultrasound Breast Elastography

Richard G. Barr, MD, PhD† and Ravi A. Managuli, PhD‡§*

Objective: Strain ratio (SR) is a semiquantitative parameter in differentiating benign from malignant tumors in breast ultrasound elastography. Currently, SR is computed manually and, thus, user dependent. The objective of this study was to evaluate the performance of a new tool assist strain ratio (ASR) and determine how it performs compared with an expert sonologist.

Methods: Ninety-one patients scheduled for breast biopsy were included in this institutional review board–approved/Health Insurance Portability and Accountability Act-compliant study. For manual strain ratio (MSR), fat and lesion were manually outlined, whereas for ASR, the clinician indicated the lesion center and the fat-to-lesion ratio is computed automatically. Three measurements were obtained for each lesion. The same raw data were used to calculate the MSR and ASR.

Results: The SR thresholds to differentiate benign from malignant tumors were determined using the Youden index. For MSR, the cutoff was 2.7, and for ASR was 2.8. The MSR showed a sensitivity of 88%, specificity of 64%, accuracy of 77%, positive predictive value of 72%, and negative predictive value of 92.1%. Corresponding ASR showed a sensitivity of 86%, specificity of 76%, accuracy of 81%, positive predictive value of 79%, and negative predictive value of 84%. The areas under the curve for the MSR and ASR were 0.83 and 0.85, respectively. The average coefficients of variation for the MSR and ASR measurements were 43% and 30%, respectively.

Conclusion: Assist strain ratio demonstrated similar diagnostic performance compared with MSR. In addition, the coefficient of variation of ASR is lower, implying lower intraoperator dependency. Thus, ASR may aid less-experienced scanners in obtaining improved results.

Key Words: breast cancer, elastography, strain ratio, strain, fat-to-lesion ratio, FLR

(*Ultrasound Quarterly* 2019;35: 82–87)

Received for publication May 10, 2018; accepted September 6, 2018.

*Southwood Imaging, Youngstown; †Northeastern Ohio Medical University, Rootstown; ‡Hitachi Healthcare Americas, Twinsburg, OH; and §University of Washington, Seattle, WA.

Hitachi provided an equipment grant to perform the study. Other disclosures: Richard G. Barr, MD, PhD—Speakers Bureau–Philips Ultrasound, Bracco Diagnostics, Lantheus Medical, Canon America. Research Grants: Philips Ultrasound, Siemens Ultrasound, GE Ultrasound, B and K Ultrasound, SuperSonic Imagine, and Bracco Diagnostics. Advisory panels: Bracco Diagnostics and Lantheus Medical. Royalties: Thieme Publishers. Ravi A. Managuli, PhD, is and employee of Hitachi Healthcare Americas.

Address correspondence to: Richard G. Barr, MD, PhD, Southwoods Imaging, 7623 Market Street, Youngstown, OH 44512 (e-mail: rgbarr@zoominternet.net).

DOI: 10.1097/RUQ.0000000000000398

Breast cancer is very prevalent among women, and in 2017 alone, 300,000 new diagnoses and 40,000 fatalities are expected in the United States.[1] To reduce the fatality rate and to identify cancer at an early stage, breast cancer screening is conducted.[2] Mammography is the modality of choice for screening breast cancer, whereas ultrasound (US) is routinely used for young women with dense breast tissue, as well as BIRADS-0 category patients, to categorize suspicious lesions found in the mammography examination and for US-guided real-time biopsy intervention.[3]

In addition to traditional grayscale and color Doppler US examinations, US-based elastography imaging is also being used to visualize stiffness of the tissue to differentiate benign from malignant tumors.[4] Both strain elastography (SE) and shear wave elastography have been used to characterize breast lesions as benign or malignant. Shear wave elastography is quantitative, whereas SE is qualitative. This study uses SE to characterize breast lesions. An example of an SE image is shown in Figure 1, where pixels with high strain (soft) are represented in red and pixels with low strain (stiff) are represented in blue. The image displayed is qualitative, implying the stiffer the lesion is, the bluer it will be. To augment the qualitative differentiation and facilitate the clinician for better differentiation of the tumor, many semiquantitative parameters can be generated based on the elastography images, including the Tsukuba score[5]; fat-to-lesion ratio (FLR), which is also called strain ratio (SR),[6] or the length size ratio of the elastographic image to the B-mode image (E/B ratio)[7]; and shear-wave speed.[8,9] By using a certain threshold, for example, 3 for the Tsukuba score and 1.0 for the E/B, a lesion is considered benign if the quantitative parameter is below the threshold, or malignant if it is greater than the threshold. The focus of this study is the enhancement made to the FLR technique to overcome existing limitations, as outlined in the next paragraph.

The FLR measurement is illustrated in Figure 2. It is the ratio of the mean strain in the fat's region of interest (ROI) (ie, sum of all strains in the fat ROI divided by the area of fat ROI) to the mean strain in the lesion's ROI (ie, sum of all strains in the lesion ROI divided by the area of lesion ROI). A low FLR implies a soft lesion, and a high FLR implies a stiff lesion. The computed FLR is then compared against a predetermined threshold FLR to differentiate between benign lesions (ie, soft) from malignant lesions (ie, hard). Many FLR thresholds have been discussed in the literature to differentiate benign from malignant lesions. Farrokh et al[10] reported a sensitivity of 94.4% and a specificity of 87.3% with a cutoff value above 2.9. Alhabshi et al[11] used a cutoff value of 5.6 for SR. Sadigh et al[12]

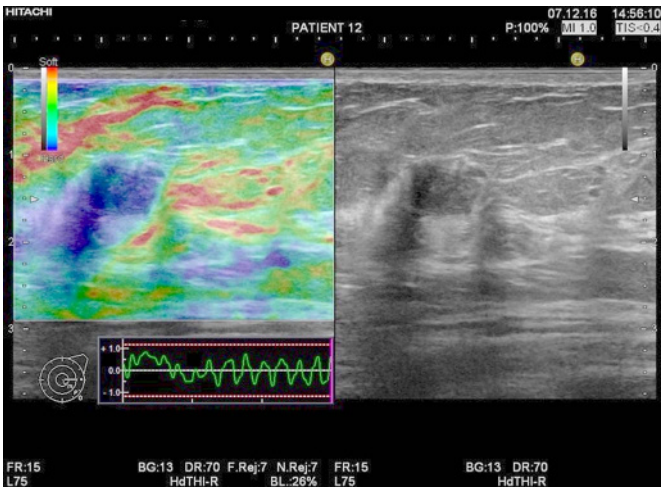

FIGURE 1. Images of an invasive ductal carcinoma with the B-mode image on the right and the strain elastogram on the left. The elastogram is color coded, with red as soft and blue as stiff. In this example, the lesion is stiff (blue). Because SE is qualitative and not quantitative, it is unknown if the lesion is stiff enough to be classified as a cancer.

demonstrated FLR utility using 3.04 as a threshold. Although FLR has been found to be very useful as a diagnostic parameter, variations in threshold across different clinical studies have lent itself to clinical decision confusion. The main reasons for these variations are 2-fold: (1) differences in breast densities specific to geographical regions, for example, Europe, Asia, and North America, and (2) the manual choice of ROI for fat and lesion by the clinicians. Although the first limitation can be addressed by performing a comprehensive clinical study specific to a region and determining the threshold, the second limitation, however, can be addressed through technology development assisting the clinicians, which would overcome one of the biggest limitations of FLR.

To overcome the variability in choosing the fat and lesion ROI by clinicians, a software called assist strain ratio (ASR) has been developed, which requires user input to select the ROI of the lesion only. The ROI of fat is automatically selected by the software without any user input. In 2014, a preliminary study was conducted in Japan using the ASR to show the efficacy of this technique.[13] Although results were promising, the software has since then been improved to overcome limitations listed in the article, including large variation at large strain values and selecting better ROI for the fat region. In this study, we describe this new technique in greater detail and conduct a clinical study to compare the effectiveness of automatically computed strain ratio (ASR) over manually computed strain ration (MSR) calculated by an expert user. Previous clinical studies were all conducted outside North America. Through this clinical study, we also establish the FLR threshold that is based on patients from North America. We compare the diagnostic performance of ASR against MSR using various statistical parameters such as positive predictive value (PPV), negative predictive value (NPV), sensitivity, and specificity. The main objective of this study was to confirm whether the performance of ASR is similar to MSR when performed by an expert user, which may aid less-experienced scanners to use this technique for improved diagnosis.

STUDY DESIGN AND PROTOCOL

Ninety-one patients scheduled for biopsy were included in this institutional review board–approved and Health Insurance Portability and Accountability Act-complaint study from August 2016 through February 2017. No inclusion/exclusion criteria were used in selecting the patient. A skilled physician (R.G.B.) performed elastography examination on all the patients. Both B-mode images and elastograms were obtained by applying minimal vibration, a technique recommended in the World Federation of Ultrasound in Medicine and Biology Guideline.[8] The stable elastography image from the acquired cine was selected on which both MSR and ASR were measured. The examination was repeated 3 times, and all 3 measurements were used as independent variables for statistical analysis. The same 3 acquisitions were used to calculate the MSR and ASR. After the final diagnoses were obtained from pathology results, statistical analysis was performed. For each lesion, FLR mean, SD, and percent coefficient of variation of the MSR and ASR values were calculated, and *P* value was analyzed.

Equipment and Software

Hitachi's HI VISION Ascendus system with EUP-L75 (linear-type probe 18–5 MHz) with experimental software to calculate the ASR was used for this study. For measuring the SR manually (MSR), a tool is available for the operator to set an ROI for the lesion as well as the subcutaneous fat. The size of the ROI was selected to include between 50% and 70% of the lesion. When possible, the fat ROI was selected at a similar depth. The fat ROI was selected so that only fat was present in the ROI. The ratio of the mean strain within each of the 2 ROIs is then computed by the software.

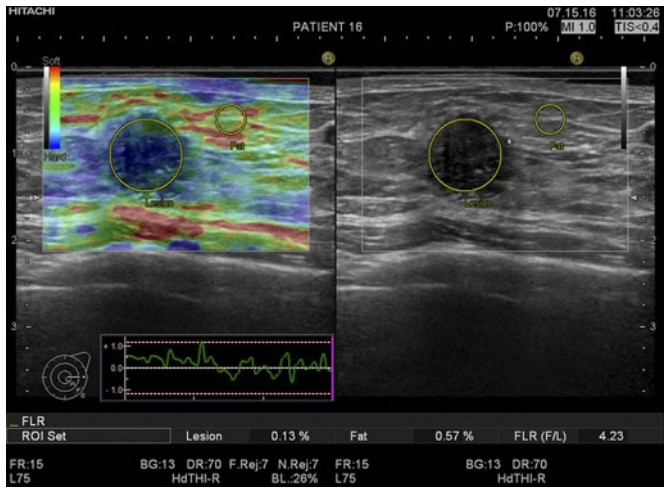

FIGURE 2. The FLR calculation is demonstrated in this case. The larger circle is placed in the lesion, whereas the smaller lesion is placed in the fat in the lesion. The strain calculations are listed in the lower portion of the image (lesion, 0.13%; fat, 0.57%). The calculated FLR is 4.23. This lesion was an invasive ductal cancer on core biopsy.

The algorithm used to calculate the ASR is as follows. The center of a lesion is specified by the user on the B-mode image (Fig. 3A), from which the system automatically calculates the gradient distribution of echo brightness (Fig. 3B) detecting the contour of the lesion border (Fig. 3C) inscribing the lesion (Fig. 3D). The algorithm is designed independent of the type and echogenicity of the lesion, that is, isoechoic or heterogeneity of the lesion. If the algorithm does not correctly outline the lesion, the user is given an option to adjust the boundary to outline the lesion appropriately (similar to manual outlining of the tumor). For selecting the fat ROI, the software automatically detects an area that does not contain low strain using the gradient distribution of echo brightness and the strain distribution information and selects the center point of the subcutaneous for fat ROI. The ROI is extended to the anterior boundary of the breast tissue (Fig. 3E). The SR is then calculated, that is, the ratio of the mean strain in the fat area to the mean strain in the lesion area.

Data Analysis

The goals of the data analysis were to demonstrate the equivalence of ASR to MSR performed by an expert user and to determine the diagnostic performance of ASR compared with MSR. After scanning the patient for lesions and identifying the best appropriate imaging plane for lesion evaluation, cine of elastography image is acquired and stored on the machine. From the acquired cine, the elastogram frame best suited for calculating ASR and MSR is selected. The MSR and ASR are calculated on the same selected elastogram (ie, image depicting the strain). The MSR was calculated first to eliminate any observer bias that would be generated if the ASR was performed first. Using the tools provided to manually outline ROIs for fat and lesion, the MSR is calculated. For ASR, after a single point is placed within the lesion (on BW-mode image), the software automatically outlines fat and lesion ROI. Three sets of data are acquired for both MSR and ASR to analyze intraobserver variability. The mean and SD were calculated for the malignant, benign, and total number of lesions, and P values (2-sided test) were evaluated by the t test. The correlation coefficients between the MSR and ASR were also calculated for the SR. A t test (2-sided test) was applied to all data in the 2 groups to calculate the P value, after confirming that the data in both groups are normally distributed, with P less than 0.05 considered statistically significant and correlation coefficient r greater than 0.6 considered high correlation. To compare the repeatability of the FLR measurement using MSR versus ASR, the coefficient of variation (COV) is computed from 3 measurements made for each patient.

To compare the diagnostic performance of MSR and ASR, sensitivity, specificity, accuracy, PPV, and NPV were calculated based on the final diagnosis of the lesions. A threshold cutoff for differentiating benign and malignant was computed by the Youth index and is subsequently used for analysis.[14] Receiver operating characteristic (ROC) curves were plotted to calculate the areas under the curve (AUCs). Statistical analysis software JMP8 (SAS Institute Inc) was used for all the analysis.

RESULTS

In total, 91 lesions were imaged, and each lesion was scanned 3 times for a total of 273 elastography images. Of these

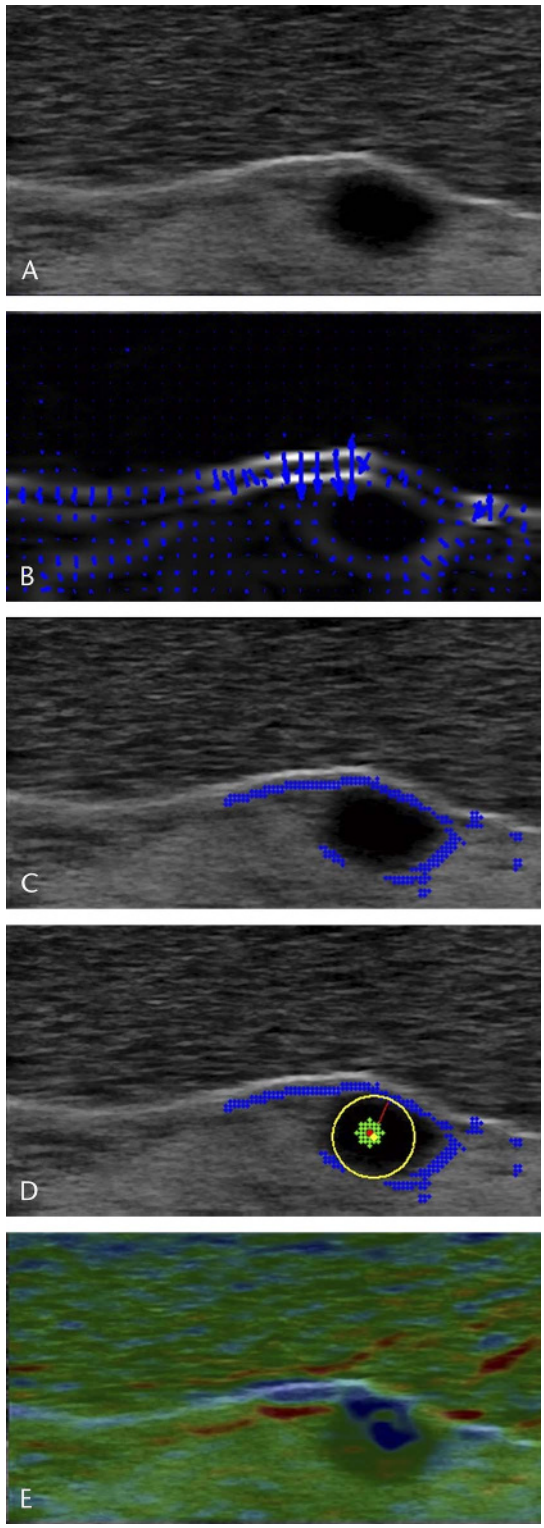

FIGURE 3. The automated SR is calculated using the following: the lesion ROI setting. A, Center of lesion specified in the BW-mode image. B, Gradient distribution of brightness. C, Lesion contour detected. D, Search edge transition. E, Auto fat ROI selection. In this method, the operator only places the curser in the center of the lesion (A) and the software automatically calculated the steps (B–E).

TABLE 1. Stain Values Obtained Manually and Automatically for Benign and Malignant Lesions

	Strain: Manual	Strain: Auto	*P*
Malignant (n = 43)	0.10 ± 0.10%	0.12 ± 0.10%	0.04
Benign (n = 42)	0.25 ± 0.20%	0.26 ± 0.19%	0.54
Total (N = 85)	0.18 ± 0.17%	0.19 ± 0.16%	0.05

91 lesions, 6 lesions were excluded from the study due to suboptimal image quality resulting from the patient breathing and depth of lesion greater than 4 cm. The remaining 85 lesions, totaling to 255 images, were subjected to statistical analysis. There were 30 invasive ductal cancers and ductal carcinoma in situ case lesions, 38 fibroadenoma/fibrocystic lesions, 4 fat necrosis, 3 papillomas, 2 each of lipoma, invasive papillary carcinoma, and signet cell carcinoma, and 1 each of intraductal papilloma, tubular carcinoma, stromal hyperplasia, hematoma, and lymph node. The mean size and SD of benign and malignant lesions were 13.5 ± 7.2 and 15.2 ± 5.8 mm, respectively, and no statistically significant difference was found in the mean size measurement ($P = 0.29$). In Table 1, mean values and SD of strains for benign (n = 42) and malignant (n = 43) tumors are tabulated. As shown in Table 1, the mean strain values for the malignant lesions in MSR and ASR were 0.1 ± 0.1% and 0.12 ± 0.1% (mean ± SD), respectively, and a statistically significant difference was found in mean strain ($P < 0.05$). Corresponding mean strain values for benign lesions with MSR and ASR were 0.25 ± 0.2% and 0.26 ± 0.19%, respectively, and no statistically significant difference was found in the mean strain ($P > 0.05$). The mean value for all lesions was 0.18 ± 0.16% with MSR and 0.19 ± 0.16% with ASR, and differences were statistically significant.

The mean SRs and SD for MSR and ASR are shown in Table 2. The MSR and ASR measurements for the malignant lesions were 6.9 ± 4.4 and 5.2 ± 2.8 (mean ± SD), respectively. For malignant lesions, a statistically significant difference was found in the mean SR ($P < 0.05$). For benign lesions, MSR and ASR measurements were 2.8 ± 2.2 and 2.5 ± 1.9, respectively, and no statistically significant difference was found in the mean SR ($P > 0.05$). The SR measurements for all the lesions were 4.9 ± 4.0 for MSR and 3.9 ± 2.7 for ASR, respectively. For all the lesions together, a significant difference was found in mean strain ($P < 0.0.05$).

To compare the intraoperator variability between ASR and MSR, 3 FLR measurements made for each patient are compared and are plotted in Figure 4. From this plot, COVs for MSR and ASR were computed and were 40.1 and 34.2, respectively.

A scatter plot showing the SR correlation between MSR and ASR is shown in Figure 5. The MSR and ASR were plotted

TABLE 2. Strain Ratios Using MSR and ASR

	SR on MSR (Mean ± SD)	SR on ASR (Mean ± SD)	*P*
Malignancy (n = 43)	6.9 ± 4.4	5.2 ± 2.8	0.005
Benign (n = 42)	2.8 ± 2.2	2.5 ± 1.9	0.180
Total (N = 85)	4.9 ± 3.9	4.0 ± 3.8	0.002

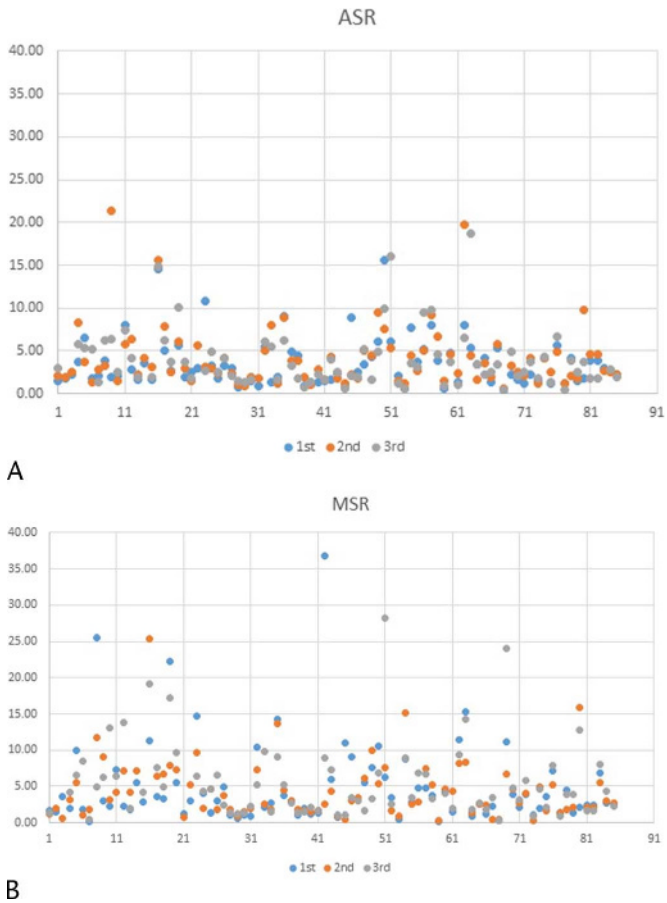

FIGURE 4. Comparing the variations in 3 FLR measurements made for each patient using the (A) MSR and (B) ASR methods. The COV computed from these 2 plots for MSR and ASR are 40.1 and 34.2, respectively.

along the *x* and *y* axes, respectively. Although there was a tendency for higher values to be more variable, the SRs for all lesions, including benign and malignant lesions, were highly correlated between the 2 groups with a positive correlation coefficient of $r = 0.70$ ($r^2 = 0.49$). Differences between MSR and ASR were statistically significant with $P = 0.001$ ($P < 0.05$). To compare the repeatability of measurements, as discussed previously, we obtained 3 SRs for each patient and each method. The ratios are plotted in Figures 4A, B for ASR and MSR, respectively. The COVs were compared from these data for MSR and ASR and were 40.1 and 34.2, respectively.

The Youden index was used to determine the optimal SR threshold for both MSR and ASR to differentiate between benign and malignant lesions.[14] In this technique, the threshold at which maximum of (sensitivity + specificity – 1) occurs is used as threshold. For ASR and MSR, thresholds of 2.8 and 2.7 were calculated, respectively. Based on these thresholds, various statistical parameters of MSR and ASR were computed and are tabulated in Table 3. The MSR showed a sensitivity of 88%, a specificity of 64%, an accuracy of 77%, a PPV of 72%, and an NPV of 92.1%. The corresponding parameter for ASR showed a sensitivity of 86%, a specificity of 76%, an accuracy of 81%, a PPV of 79%, and an NPV of 84%.

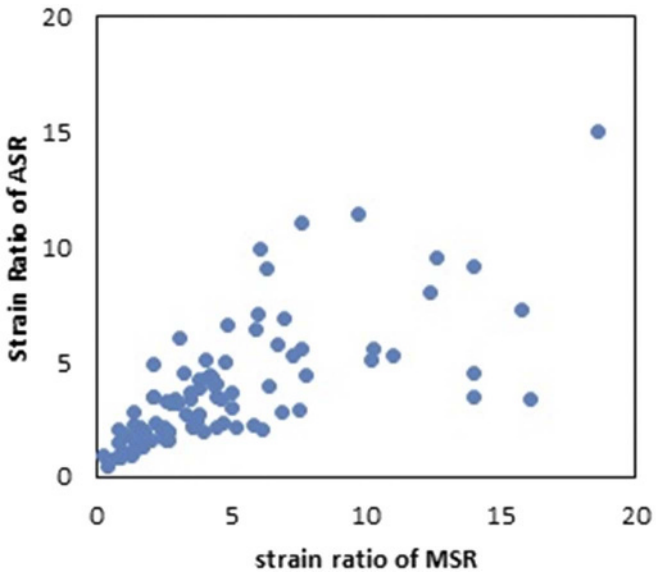

FIGURE 5. A scatter plot showing the SR correlation between MSR and ASR, which are plotted along the *x* and *y* axes, respectively. The positive correlation coefficient between MSR and ASR is $r = 0.70$ ($r^2 = 0.49$).

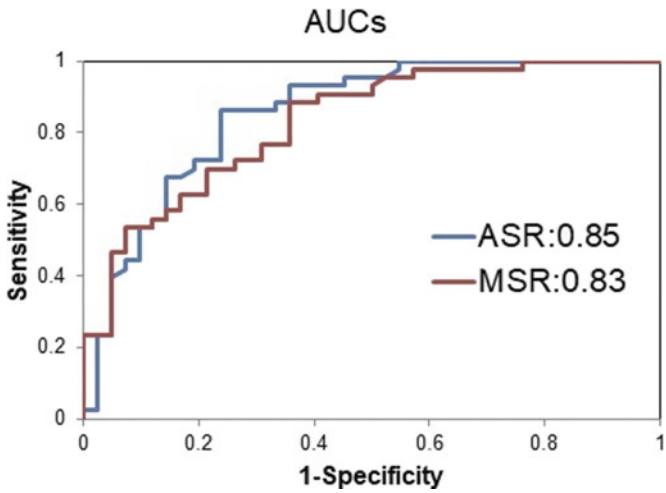

FIGURE 6. Receiver operating characteristic curves for both MSR (red) and ASR (blue) to calculate the AUCs. The AUCs for MSR and ASR were 0.83 and 0.85, respectively.

The ROC curves are plotted in Figures 5, 6 for both MSR and ASR, respectively, to calculate the AUCs. The AUCs for MSR and ASR were 0.83 and 0.85, respectively.

DISCUSSION

As can be seen from Table 3, except sensitivity, where ASR (86%) is marginally lower than MSR (88%), the diagnostic performance of ASR is equivalent or better than MSR in almost all diagnostic categories. In addition, the AUC of ASR is 0.85, which is better, compared with 0.75 of MSR. Thus, we believe that ASR can be easily adopted in daily clinical practice instead of MSR with high level of confidence. Because ASR eliminates many manual steps needed to compute SR, for example, outlining of the lesion and selecting the region of fat for computing the ratio, the test-retest capability of ASR would ideally be high compared with MSR, as it is evident from the COV of ASR being 0.3 and that of MSR being 0.45.

We compared the average strain values and SRs obtained both manually and automatically (Tables 1 and 2). For malignant lesions, mean values of automatically derived and manually derived strains and SR were statistically significant ($P < 0.05$). However, for benign lesions, average strains were not statistically significant ($P > 0.05$). Because we used the same elastogram for both automatic and manual methods, the source of variation between MSR and ASR would be from how the user outlined the ROI versus how the software outlined the ROI with minimal user input. Because ASR's specificity, PPV, NPV, accuracy, and ROC are better than those of MSR, this suggests that ASR could do a consistent and reliable ROI delineation compared with MSR. Although the clinicians had the option to adjust the ROI of fat or lesion while using the software, the clinician did not modify the ROI of any of the 85 lesions outlined by the software. Therefore, it is safe to assume that the composition of the malignant and fat lesions in addition to heterogeneity of the lesions outlined by the ASR was acceptable to the clinician.

TABLE 3. Diagnostic Performances of ASR and MSR

	Cutoff	Sensitivity	Specificity	Accuracy	PPV	NPV
MSR	2.65	88%	64%	77%	72%	84%
ASR	2.84	86%	76%	81%	79%	84%

The optimum thresholds determined using the Youden index for MSR and ASR are slightly different for the same patient population, that is, 2.7 for MSR versus 2.8 for ASR. Because ASR diagnostic performance is equivalent and/or superior to MSR, the threshold determined for ASR can be used as a standard threshold while using SR. In due course, finer adjustments could be made to this threshold, as more clinical studies are conducted and/or more clinical information is incorporated. The threshold of 2.8 determined in this study is similar to the threshold of 2.9 determined by Farrokh et al[10] and the 3.04 determined by Sadigh et al.[12] However, it is significantly different from the threshold of 5.7 determined by Alhabshi et al.[11] These differences confirm that ASR could avoid some differences arising due to the technique used, but geographical region–based differences in breast tissue characteristics could still dominate in determining the global threshold. Other possible explanations for the difference in cutoff values are different degrees of precompression[15] used and variability of how each vendor estimates strain from the images.[8] If the clinician is not careful with precompression, the stiffness values of all the tissues are increased artificially with fat stiffness increasing at a higher rate than other tissues.[15]

When we compare our diagnostic performance to the article published in 2014 in Japan using the ASR technique,[13] our ASR is better than MSR, whereas in 2014, MSR was better than ASR. In addition, the correlation between MSR and ASR in 2014 was less than 0.5, whereas in our current study, it is more than 0.7. Thus, whereas the 2014 article showed the feasibility

of ASR, our current study establishes that the ASR software is more reliable and could be used readily by clinicians.

Because the ROI of a lesion is calculated with minimal user input and fat ROI is automatically calculated, the user dependence on SR computation using ASR reduces significantly. However, the frame on which these values are computed still depends on the frame selected by the user, which could introduce some variability. Recently, Hitachi introduced a new software called Auto Frame Select, which facilitates automatic selection of the optimal frame based on strain distribution.[13] This technique was not evaluated in this study. We also did not do interoperator dependency and only addressed intraoperator dependency. In the next planned clinical study, we will use Auto Frame Select, multiple users, and the threshold determined in this study to address interoperator dependency. We also did not perform a multivendor study. Thus, the threshold determined in this study is limited to the Hitachi system only. In the absence of recommendations from other vendors, the threshold determined in this study could be used for other systems as a baseline, with subsequent fine-tuning to accommodate vendor differences in implementing elastography and SR computations. We also did not compare our results against shear-wave and B/A ratio technique to see how well ASR would perform against those techniques. This will be the topic of our next clinical study as well.

CONCLUSION

The diagnostic performance and ROC analysis of ASR were equivalent or better than MSR, demonstrating the feasibility of using software-assisted SR computation rather than manually computed SR. In addition, because the software-assisted technique only requires the identification of the lesion by the clinician and placing of a small circle at the center, it could potentially reduce inter- and/or intraobserver dependency, as is evident from the reduced COV of ASR. We also established an SR threshold of 2.8, which can be used to differentiate benign from malignant lesions. As a next step, we plan to include multiple clinicians and more patients to perform an intra- and interobserver variability study.

ACKNOWLEDGMENT

We thank Koji Waki of Hitachi Healthcare, Japan, for providing technical assistance.

REFERENCES

1. Cancer.org, B. US Breast cancer statistics. Available at: http://www.breastcancer.org/symptoms/understand_bc/statistics. Accessed June 2017.
2. Smith RA, Andrews KS, Brooks D, et al. Cancer screening in the United States, 2017: a review of current American Cancer Society guidelines and current issues in cancer screening. *CA Cancer J Clin*. 2017; 67(2):100–121.
3. Lee CH, Dershaw DD, Kopans D, et al. Breast cancer screening with imaging: recommendations from the Society of Breast Imaging and the ACR on the use of mammography, breast MRI, breast ultrasound, and other technologies for the detection of clinically occult breast cancer. *J Am Coll Radiol*. 2010;7(1):18–27.
4. Krouskop TA, Wheeler TM, Kallel F, et al. Elastic moduli of breast and prostate tissues under compression. *Ultrason Imaging*. 1998;20(4):260–274.
5. Itoh A, Ueno E, Tohno E, et al. Breast disease: clinical application of US elastography for diagnosis. *Radiology*. 2006;239(2):341–350.
6. Ueno E, Tohno E, Soeda S, et al. Dynamic tests in real-time breast echography. *Ultrasound Med Biol*. 1988;14(suppl 1):53–57.
7. Barr RG. Real-time ultrasound elasticity of the breast: initial clinical results. *Ultrasound Q*. 2010;26(2):61–66.
8. Barr RG, Nakashima K, Amy D, et al. WFUMB guidelines and recommendations for clinical use of ultrasound elastography: part 2: breast. *Ultrasound Med Biol*. 2015;41(5):1148–1160.
9. Berg WA, Cosgrove DO, Doré CJ, et al. Shear-wave elastography improves the specificity of breast US: the BE1 multinational study of 939 masses. *Radiology*. 2012;262(2):435–449.
10. Farrokh A, Wojcinski S, Degenhardt F. Diagnostic value of strain ratio measurement in the differentiation of malignant and benign breast lesions. *Ultraschall Med*. 2011;32(4):400–405.
11. Alhabshi SM, Rahmat K, Abdul Halim N, et al. Semi-quantitative and qualitative assessment of breast ultrasound elastography in differentiating between malignant and benign lesions. *Ultrasound Med Biol*. 2013;39(4): 568–578.
12. Sadigh G, Carlos RC, Neal CH, et al. Ultrasonographic differentiation of malignant from benign breast lesions: a meta-analytic comparison of elasticity and BIRADS scoring. *Breast Cancer Res Treat*. 2012;133(1):23–35.
13. Healthcare H. Available at: http://www.hitachi.com/ultrasound/. Accessed June 2017.
14. Ruopp MD, Perkins NJ, Whitcomb BW, et al. Youden index and optimal cut-point estimated from observations affected by a lower limit of detection. *Biom J*. 2008;50(3):419–430.
15. Barr RG, Zhang Z. Effects of precompression on elasticity imaging of the breast: development of a clinically useful semiquantitative method of precompression assessment. *J Ultrasound Med*. 2012;31(6):895–902.